CFD Modeling of Three-phase Bubble Column: 1. Study of Flow Pattern

M. Anil, V. K. Agarwal, M. Siraj Alam, and K. L. Wasewar*
Chemical Engineering Department, Indian Institute of Technology (IIT),
Roorkee – 247667, Uttarakhand, India
Email: k_wasewar@rediffmail.com, klw73fch@iitr.ernet.in
Phone: +91-1332-285347; Fax: +91-1332-276535

Original scientific paper
Received: August 28, 2006
Accepted: March 1, 2007

Bubble column (BC) or slurry bubble column (SBC) reactor has emerged as one of the most promising devices in chemical, biochemical and environmental engineering operations because of its simple construction, isothermal conditions, high heat and mass transfer rates, and on-line catalyst addition and withdrawal. The present work has been carried out to characterize the dynamics of three-phase flow in cylindrical bubble column, run under homogeneous bubble flow and heterogeneous flow conditions using CFD (Computational Fluid Dynamics) simulation. The investigation has been done to study the flow pattern of three-phase bubble column along with parametric studies. The simulations were performed for air-water-glass beads in a bubble column of H = 0.6 m height, D_i = 0.1 m and d_s = 0.05 m sparger diameter to study the flow pattern. Eulerian-Eulerian three-phase simulations with k-ε turbulence for liquid phase were carried out using the commercial flow simulation software CFX-5.6, with a focus on characterizing the dynamics properties of gas liquid solid flows. The model has been validated using available experimental data and is in good agreement. Detail study of the flow pattern in three-phase bubble column has been carried out and flow pattern has been presented in the form of contour and vector plots. The results presented are useful for understanding the dynamics of gas liquid solid flows in bubble column and provide a basis for further development of CFD model for three phase systems.

Key words:
CFD, Bubble column, Euler-Euler model, three phase reactor

Introduction

Bubble column (BC) or slurry bubble column (SBC) reactor has emerged as one of the most promising devices in chemical, biochemical and environmental engineering operations because of its simple construction, isothermal conditions, high heat and mass transfer rates, and on-line catalyst addition and withdrawal. In bubble column slurry reactors, a gas is dispersed through a deep pool of liquid containing suspended solid particles. In these reactors, the momentum is transferred to the liquid phase and solid phase by the movement of the gas bubbles. Bubble column reactors have a wide range of applications such as absorption, catalytic slurry reactions, bioreactions, coal liquifications etc. Bubble (slurry) reactors are used extensively to carry out a variety of gas liquid and gas liquid solid reactions. Classic examples are carbonation of lime slurry, chlorination of paper stock, hydrogenation of vegetable oils, aeration of fermentation broths as in the production of penicillin, production of citric acid from sugar by action of microorganisms, and the aeration of activated sludge for biological oxidation etc. Bubble columns are preferred over other multiphase reactors because it requires less maintenance due to absence of moving parts, and it also provides higher values of effective interfacial areas, overall mass transfer coefficients, higher heat transfer rates per unit volume of the reactor, and easy solids handling without any erosion or plugging problems. At the same time these types of reactors are cheaper and require less floor space, and can easily accommodate slow reactions due to high liquid residence time.

Computational Fluid Dynamics (CFD) is the science of predicting fluid flow, heat transfer, mass transfer, chemical reactions, and related phenomena by solving the mathematical equations that govern these processes using numerical algorithms. The results of CFD analysis are relevant engineering data used in conceptual studies of new designs, detailed product development, troubleshooting, and redesign and therefore CFD is gaining importance in general process applications. CFD approaches use numerical techniques to solve the Navier-Stokes equations for given flow geometry and boundary conditions thereby implementing models for flow aspects like

* Corresponding author

turbulence or heat and mass transfer as relevant for the specific modeling task. It has also been an important tool in air and space industry as well as vehicle design for a long time where it deals with a large extent replaced time-consuming and expensive wind tunnel experiments. Although, these applications are of single-phase flow, but most of the applications in chemical and biochemical reactors includes multiphase flow and modeling and numerical treatment of those introduce additional challenges. Therefore, multiphase CFD applications have gained broad attention during the last decade with enhanced computational. Although, most of the literatures available are limited to two-phase flows, and especially gas-liquid CFD projects often deal only with very low dispersed phase holdups. In effect this means that multiphase CFD still is far away from being a general tool for the practitioner even if recent advances in computational power available in desktop PCs do enable first steps in this direction.

Bubble columns have been studied extensively in literature, and many investigators have reported results on CFD simulations. *Pfleger* et al.[1] investigated behavior of a flat laboratory-scale rectangular two-phase bubble column using the Euler-Euler approach by the help of CFX-4.2 and found that 2D modeling of a flat bubble column is not possible. This result is supported by the work of *Sokolichin* and *Eigenberger*[2]. They used in-house CFD code but were unable to implement that for three-dimension. Both of these studies were carried out at extremely low superficial gas velocities (below 0.01 m s^{-1}). *Krishna* et al.[3] reported CFD based modeling of a pilot-plant size bubble column using CFX-4.2 with the Euler-Euler model as well as at higher superficial gas velocities (up to u = 0.28 m s^{-1}). While one of their reports is entitled "*Three-Phase Eulerian Simulation*" the reader would be misled to assume that they included solid particles into their considerations; moreover, two dispersed gas phases were calculated to include the different influences of large and small bubbles. In addition, they calculated integral gas holdups and derived a scale-up correlation for bubble columns of different sizes. Sparger influence on the flow structure in two-phase bubble columns with a low height-to-diameter ratio of two was the aim of investigations carried out by *Ranade* and *Tayalia*[4]. Using the commercial code Fluent 4.5.2 with an Euler-Euler approach implementing the k-ε model and in agreement with measurement results they found that single ring spargers induce a characteristic liquid circulation, which can not be observed in a double-ring sparger configuration. Three-dimensional calculations could not be avoided for a correct prediction of flow fields. Three-phase CFD modeling results were presented for bubble columns by *Mitra-Majumdar* et al.[5] and for airlift loop reactors by *Padial* et al.[6] While the first group reports results obtained from two-dimensional calculations in cylindrical coordinates, the latter had to perform full three-dimensional calculations to achieve useful results.

Further, *Michele* and *Hempel*[7] reported detailed measurements of local dispersed phase holdups in a pilot plant-sized bubble column operated at high superficial gas velocities and solid holdups. It deals with the influence of superficial gas velocity, solid loading and sparger geometry on measured and computed liquid flow velocities and holdup distributions. Liquid velocity measurements have been performed using the electrodiffusion method; modeling calculations have been carried out using the computational fluid dynamics (CFD) code CFX-4.3. The experimental setup used by them consisted of a pilot plant-sized bubble column (inner diameter D_i = 0.63 m, height H = 6 m) made from plexiglass which could be equipped with a plate sparger, a ring sparger or a central nozzle. Probe ports allowed for the introduction of measurement equipment at a vertical spacing of h = 0.5 m, starting 0.35 m above the sparger level. Their measurements were taken at seven radial positions for each level, ranging from reactor centre to reactor edge (spacing 0.05 m. The investigated three-phase system consisted of de-ionized water supplemented with potassium sulphate at a concentration of c = 0.01 mol l^{-1}, air and plexiglass granules (polymethyl-methacrylate, PMMA, density ρ = 1200 kg m^{-3}, particle hydraulic diameter d_p = 0.003 m). The solid material was chosen as the model system to represent particles with a biofilm growing on them as employed in biotechnological applications. Solid loadings were varied from φ = 0 % (two-phase flow) to φ = 10 %, superficial gas velocities ranged from u = 0.02 to 0.09 m s^{-1}.

It is evident from the previous discussion that the flow patterns in the bubble column and flow parameters have lot of importance for the overall column performance. Hence, it is essential to understand the hydrodynamics of the bubble column. It is also clear from above that most literature reported are limited to two-phase flows, and especially gas-liquid CFD projects often deal only with very low dispersed phase holdups, in spite of increased computational power available for the multiphase CFD applications. In the present paper, the flow pattern in a bubble column using CFD based software CFX-5.6, has been studied.

Mathematical modeling

Multiphase CFD modeling, mainly classified into two approaches Eulerian-Eulerian and Eulerian--Lagrangian based on dispersed phase (particles, droplets or bubbles) handling considerations. The former approach assumes that the dispersed phase consits of representative particles transported with the continuous phase. A set of Navier-Stokes equations is solved only for the continuous phase; coupling between the motion of the continuous and the dispersed phases and thus computation of the particle motion is achieved by tracking the particles via drag law considerations. The Eulerian-Eulerian or multi-fluid approach assumes the dispersed and continuous phases to be interpenetrating continua, for both of which a complete set of Navier-Stokes equations has to be solved. Coupling between the motion of the dispersed and the continuous phase is achieved by implementing momentum exchange terms into the respective phase's momentum balance equations; these terms are usually based on drag considerations as with the Eulerian Lagrangian approach.

The Eulerian-Eulerian approach has been chosen for present study because of its obvious computational advantages at high dispersed phase contents: While in Eulerian–Lagrangian approach suffers from high demands on computational power; this renders them rather unsuitable for the computation of multiphase flows in real process applications where dispersed phase holdups are usually high. Therefore, in this present study the Euler-Euler or multi-fluid approach will be implemented which allows for the computation of three-phase flow fields even with high solid and gas holdups at reasonable computational expense.

Hydrodynamic model

Assumptions

The following assumptions are made for hydrodynamic modeling of bubble column:

– 3D, transient as well as steady state.

– Isothermal flow conditions, so no energy equations.

– Mass transfer and chemical reactions have been neglected.

– Buoyancy effect was included in order to correctly model bubble rise.

– Liquid phase turbulence was modeled using the k-ε model; the dispersed phases were considered laminar.

– The system of equations was solved using a finite-volume scheme.

– Momentum transfer between the liquid and the dispersed phases was modeled using the appropriate drag laws for the respective flow regime.

– Momentum transfer between the dispersed phases were neglected.

– Bubbles are assumed as rigid sphere having a constant diameter.

Conservation of mass: continuity equation

The continuity equation describes the mass flux into and out of a control volume. The continuity equations for continuous as well as dispersed phase are as follows:

$$\frac{\partial(\varepsilon_\alpha \rho_\alpha)}{\partial t} + \nabla(\varepsilon_\alpha \rho_\alpha v_\alpha) = 0 \tag{1}$$

where α = 1, 2, 3

ε_α is the volume fraction of phase α, and

$$\sum_\alpha \varepsilon_\alpha = 1 \tag{2}$$

Conservation of momentum: equation of motion

In multiphase formulation, momentum balances look slightly different for continuous and dispersed phases. The momentum balance for the continuous phase in most general formulation is:

$$\frac{\partial(\varepsilon_\alpha \rho_\alpha v_\alpha)}{\partial t} + \nabla^2(\varepsilon_\alpha \rho_\alpha v_\alpha v_\alpha) =$$

$$= -\varepsilon_\alpha \nabla p_\alpha + \nabla(\varepsilon_\alpha \mu_\alpha(\nabla v_\alpha + (\nabla v_\alpha)^T)) + \tag{3}$$

$$+\varepsilon_\alpha \rho_\alpha g + M_\alpha$$

Momentum exchange between continuous and dispersed phase i.e. liquid-gas and liquid-solid is:

$$M_\alpha = \sum_{\beta=1}^{N_p} c_{\alpha,\beta}(v_\beta - v_\alpha) \tag{4}$$

where

$$c_{\alpha,\beta} = \frac{3}{4}\frac{C_D}{d_p}\varepsilon_\beta \rho_\beta |v_\beta - v_\alpha| \tag{5}$$

Momentum balance for the dispersed phase is:

$$\frac{\partial(\varepsilon_\beta \rho_\beta v_\beta)}{\partial t} + \nabla^2(\varepsilon_\beta \rho_\beta v_\beta v_\beta) =$$

$$= -\varepsilon_\beta \nabla p_\beta + \nabla(\varepsilon_\beta \mu_\beta(\nabla v_\beta + (\nabla v_\beta)^T)) + \tag{6}$$

$$+\varepsilon_\beta \rho_\beta g + M_\beta$$

Momentum exchange between continuous and dispersed phase i.e. liquid-gas for gas phase and liquid-solid for solid phase is:

$$M_\beta = c_{\alpha,\beta}(v_\beta - v_\alpha) \tag{7}$$

where

$$c_{\alpha,\beta} = \frac{3}{4}\frac{C_\mathrm{D}}{d_\mathrm{p}}\varepsilon_\beta \rho_\beta |u_\beta - u_\alpha| \tag{8}$$

For liquid-gas,

$$C_D = 0.44 \qquad Re > 1000 \tag{9}$$

and for liquid-solid,

$$c_\mathrm{D} = \frac{24}{Re}(1 + 0.15\mathrm{Re}^{0.687}) \qquad Re \le 1000 \tag{10}$$

Turbulence Modeling

Turbulence modeling is of crucial importance for the correct description of multiphase flows in CFD modeling. In this study, one of the most prominent turbulence models, standard k-ε model was considered which has been implemented in most general purpose CFD codes and is considered the industry standard model. It has proven to be stable and numerically robust and has a well-established regime of predictive capability. For general purpose simulations, the k-ε model offers a good compromise in terms of accuracy and robustness.

Since in the computations carried out here the liquid phase is the continuous one, the conservation equation for the liquid turbulent kinetic energy k may be written as follows:

$$\frac{\partial}{\partial t}(\varepsilon_l \rho_l k) + \frac{\partial}{\partial t}(\varepsilon_l \rho_l u_{l,j} k) - \\ -\frac{\partial}{\partial x_i}\left(\varepsilon_l\left(\mu_{l,\mathrm{lam}} + \frac{\mu_{l,\mathrm{turb}}}{\sigma_\varepsilon}\right)\frac{\partial k}{\partial x_i}\right) = \\ = \varepsilon_l(G - \rho_l \varepsilon) + S_{l,k} \tag{11}$$

Here, G is a turbulence production term and S_{lk} is a source term; both of these may be used to e.g. implement turbulence effects of bubbles or particles but are not considered here and thus set to zero.

The conservation equation for the liquid turbulent dissipation ε is:

$$\frac{\partial}{\partial t}(\varepsilon_l \rho_l \varepsilon) + \frac{\partial}{\partial t}(\varepsilon_l \rho_l u_{l,j} \varepsilon) - \\ -\frac{\partial}{\partial x_i}\left(\varepsilon_l\left(\mu_{l,\mathrm{lam}} + \frac{\mu_{l,\mathrm{turb}}}{\sigma_\varepsilon}\right)\frac{\partial \varepsilon}{\partial x_i}\right) = \\ = \varepsilon_l(C_{g1}G - C_{g2}\rho_l \varepsilon) + S_{l,\varepsilon} \tag{12}$$

The source term $S_{l\varepsilon}$ is set to zero as with $S_{l,k}$.

The effective liquid dynamic viscosity is combined for the turbulent case from a laminar and a turbulent part:

$$\mu_\alpha = \mu_{\alpha,\mathrm{lom}} + \frac{\mu_{\alpha,\mathrm{turb}}}{\sigma_k} \tag{13}$$

Where the turbulent viscosity $\mu_{\alpha;\mathrm{turb}}$ is computed from:

$$\mu_{\alpha,\mathrm{turb}} = C_\mu \rho_l \frac{\mu_{\alpha,\mathrm{turb}}}{\varepsilon} \tag{14}$$

In effect, this means that with the k-ε model, three additional unknowns (k, ε and $\mu_{\alpha.\mathrm{turb}}$) and three equations (two partial differential equations, one algebraic equation) have been introduced into the calculation yielding a closed model.

Initial and boundary conditions

In order to obtain a well-posed system of equations, reasonable boundary conditions for the computational domain have to be implemented.

– With the three-dimensional calculations carried out in this project, no symmetry conditions as with 2D models were needed.

– At the walls, a no-slip boundary condition was implemented for liquid phase and free slip for gas and solid phase.

– For liquid and solid phase, reactor bottom and top were considered as walls, while the gaseous phase was allowed to enter through a patch at the reactor bottom the shape of which depended on the sparger geometry.

– The sparger cannot be modeled with all its holes but has to be modeled as a flat surface where a constant normal gas velocity and gas holdup can be prescribed. In reality, however, the local gas velocity at the small sparger holes is substantially higher leading to a better fluidization of solid particles than in the model case.

– At the reactor top, a special degassing boundary was set up where air and excess liquid or solid were allowed to leave the reactor ("overflow").

– Transient calculations started from assuming fully fluidized state with an integral gas holdup of φ = 5 % and integral solid loading according to the desired value in the calculation (i. e. φ = 0.5 or 10 %).

Results and discussion

In the present work, the flow in three phase Bubble Column was modeled using the Eulerian--Eulerian model incorporated in CFX-5.6. The de-

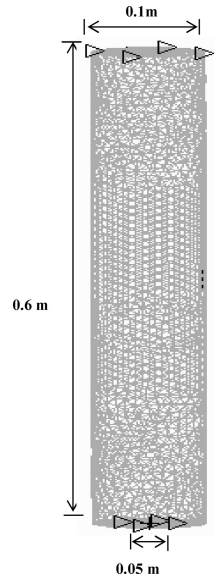

Fig. 1 – *Unstructured tetrahedral mesh for bubble column*

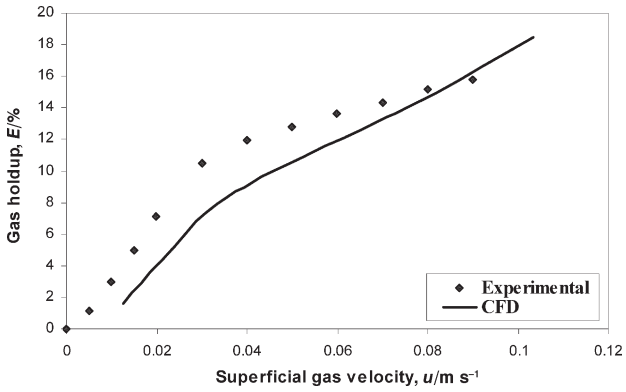

Fig. 2 – *Comparison of computed and measured gas holdup*

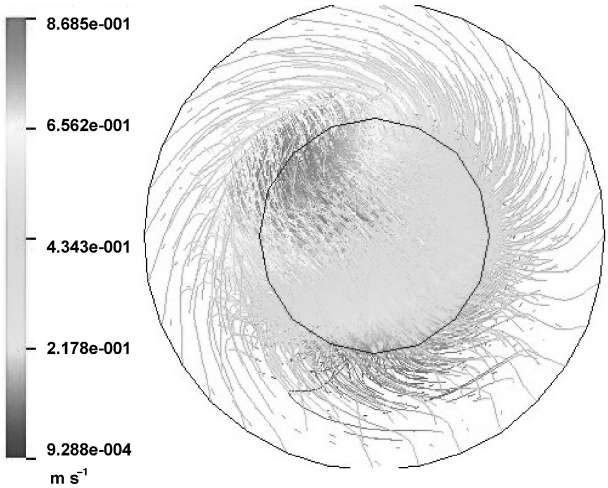

Fig. 3 – *Streamline plot of gas velocity at sparger*

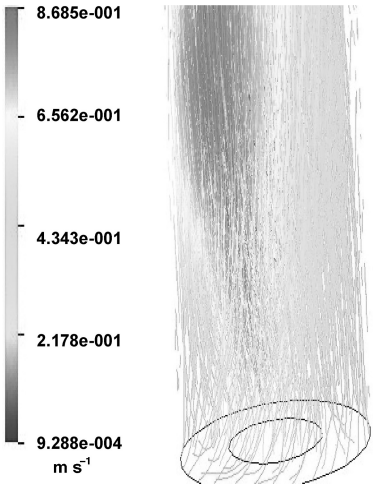

Fig. 4 – *Streamline plot of gas velocity at bottom*

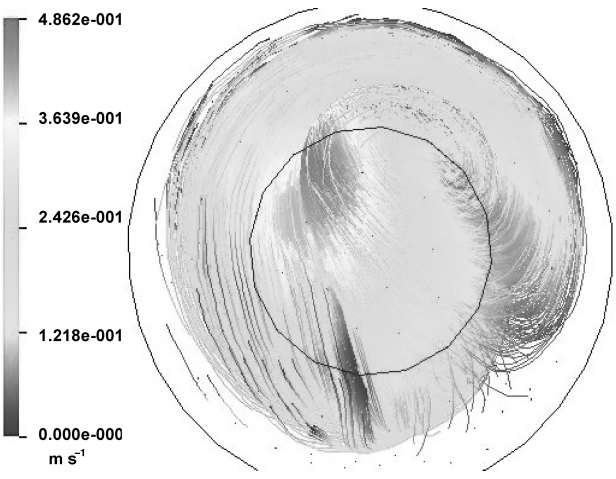

Fig. 5 – *Streamline plot of liquid velocity at bottom*

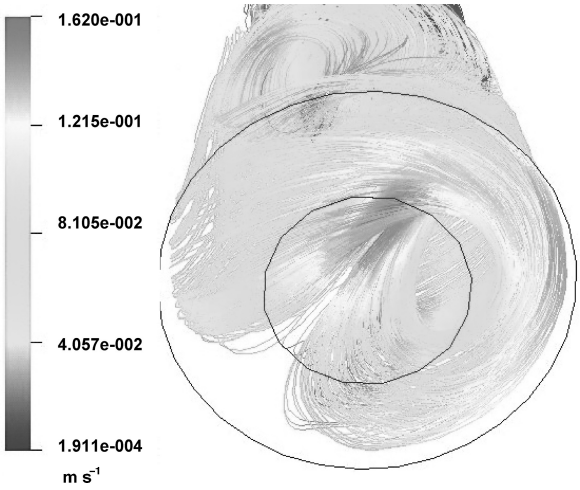

Fig. 6 – *Streamline plot of solid velocity at bottom*

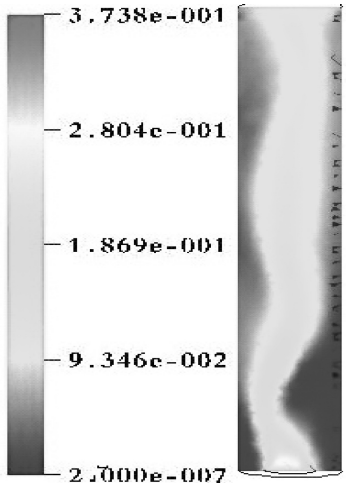

Fig. 7 – *Contour plot of gas volume fraction*

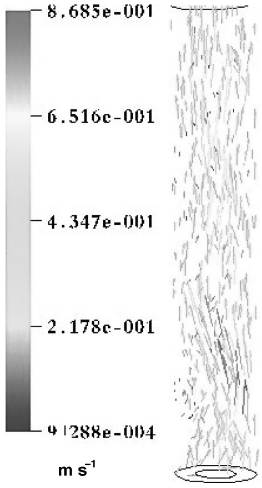

Fig. 8 – *Vector plot of gas velocity*

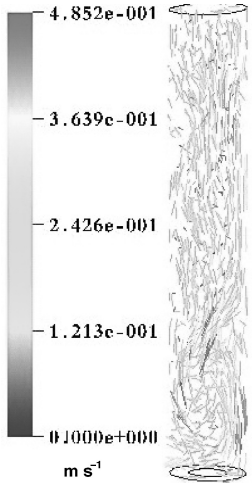

Fig. 9 – *Vector plot of liquid velocity*

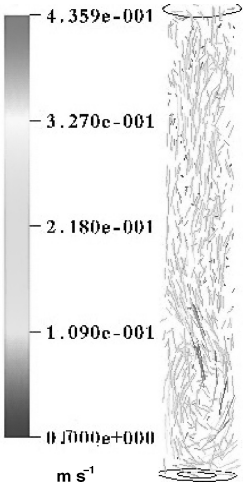

Fig. 10 – *Vector plot of solid velocity*

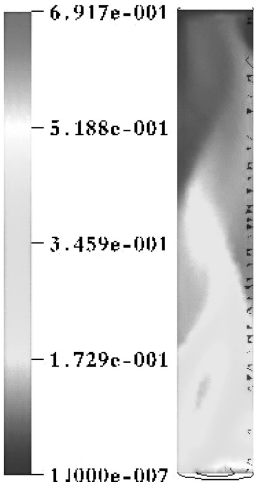

Fig. 11 – *Contour plot of solid volume fraction*

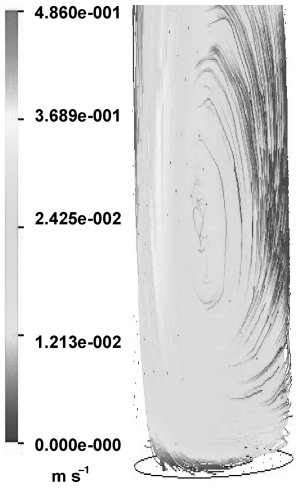

Fig. 12 – *Streamline plot of liquid velocity at sparger*

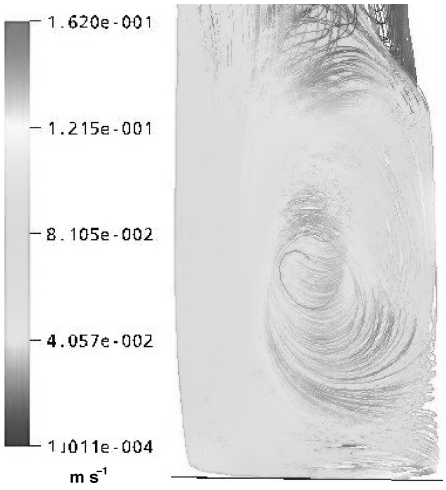

Fig. 13 – *Streamline plot of solid velocity at sparger*

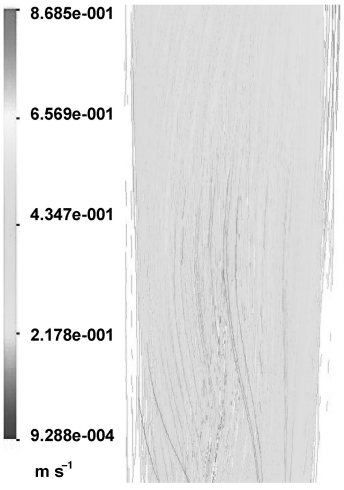

Fig. 14 – *Streamline plot of gas velocity at center*

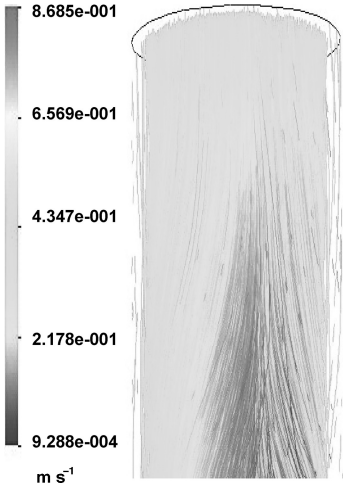

Fig. 15 – *Streamline plot of gas velocity at top*

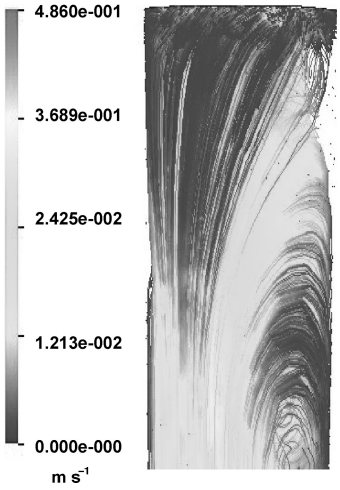

Fig. 16 – *Streamline plot of liquid velocity at top*

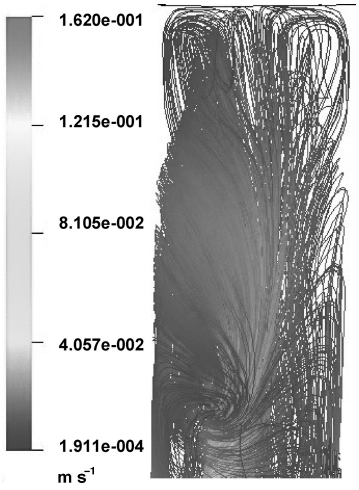

Fig. 17 – *Streamline plot of solid velocity at top*

Table 1 – *The standard reactor geometry used to study the flow pattern in bubble column*

Bubble column height, H	0.6 m
Bubble column diameter, D	0.1 m
Plate sparger diameter, d_s	0.05 m
Gas velocity, u	0.6 m s^{-1}
Solid loading, φ	10 %
Average mesh width / grid cell edge length	1 cm
Reference Pressure, p_{ref}	1 bar

Table 2 – *The three phases in the system in bubble column*

Material	Morphology	Diameter, d/mm	Density, ρ/kg m^{-3}
Air	Dispersed fluid	5	1.185
Water	Continuous fluid	–	997.0
Glass beads	Dispersed solid	1	1200

Table 3 – *Range of process variables used*

Inlet gas velocity, m s^{-1}	0.06, 0.08, 0.1, 0.2, 0.4, 0.6, 0.8, 1
Solid loading, %	0, 5, 10, 15, 20
Particle diameter, d_p/mm	0.2, 0.4, 0.6, 0.8

Table 4 – *Range of design variable used*

H/D ratio	2, 4, 6, 8, 10, 12, 14
Sparger diameter, d_s/cm	2, 4, 5, 6, 8
Taperness, d_{out}/d_{inl}	1, 1.2, 1.4, 1.6, 1.8, 2

tails of the standard geometry and three phase system used to study the flow pattern are given in Table 1 and Table 2 respectively. Unstructured tetrahedral mesh was generated for bubble column and surface mesh is shown in Fig. 1. The range of process variables and design variables used for the parametric sensitivity studies are given in Table 3 and Table 4 respectively.

Model validation

For a better quantitative assessment, which more clearly shows possibilities and limitations of the model, integral gas holdup has been computed for all the calculations presented as well and can easily be compared to experimental results of *Michele* and *Hempel*.[7] Fig. 2 shows a comparison of computed and measured integral gas holdups for bubble column height of 5 m, diameter H = 0.63 m, sparger diameter D = 0.57 m, and solid loading φ = 10 %. Agreement between measurement and modeling results with respect to integral gas holdup is quite good. While the model is capable of capturing the right order of magnitude of gas holdup and general dependency of gas holdup on superficial gas velocity, it cannot account for the different flow regimes observed in the measurements. While measurement data clearly show the division line between homogeneous and heterogeneous flow regime at a superficial gas velocity of approximately u = 0.03 m s^{-1} (marked by a distinct decrease of the graph's slope), the modeling calculations yield a slightly linear relation between superficial gas velocity and integral gas holdup for the whole range under consideration, where agreement with the experimental data is best at very low and very high superficial gas velocities. This could be due to non-inclusion of magus force and effect of surface tension. Thus, further model improvements are needed to deal primarily with correctly covering the

different flow regimes, e.g. by implementing models for bubble size distribution depending on the superficial gas velocity. The similar type of limitations was observed in computation of local liquid flow velocities. The similar results were obtained by *Michele* and *Hempel*.[7]

Flow pattern in three-phase bubble column

The simulation starts with gas injection through the sparger. The liquid and solid phase was at rest at that moment. After few seconds liquid velocity in most parts of reactor was greater than zero. It can be seen from Fig. 3 and Fig. 4 that how the gas bubbles enters the slurry at sparger position. The gas bubbles start rising to the surface as a reaction to upward directed forces. Buoyancy and drag forces are the two main components of the vertical force balance. The movement of the slurry phase is a result of the acting drag forces to the fluid elements. After the surface break-through as seen in Fig. 5 and Fig. 6, the bubble swarm stays quite in the centre of the column for a while. The bubble swarm begins its swinging after a certain start period as seen in Fig. 7. This specific movement cannot be covered by two-dimensional simulation. The simulation results showed in Fig. 8, 9, and 10 are a dynamic behavior of the flow with several circulation zones and wavy motion of bubble swarm. It was observed from Fig. 11 that solid particle concentration decrease with height of bubble column because of the action of sedimentation process on solid particle, the higher particle concentration prevails at the bottom. At lower region of bubble column there is a circulation zone of liquid and solid phase as seen in Fig. 12 and 13. At the centres in Fig. 14, there is a wavy motion of bubble swarm and at the upper region as shown in Fig. 15, 16, and 17, liquid and solid phase is circulated back into the bubble column and air is allowed to pass through the top due to degassing boundary condition. The results presented are useful for understanding the dynamics of gas liquid solid flows in bubble column and provide a basis for further development of CFD model for three phase systems

Conclusion

The need to establish a rational basis for the interpretation of the interaction of fluid dynamic variables was the primary motivation for active research in the area of bubble column modeling based on computational fluid dynamics (CFD) tools in the last decade. An appropriate mesh and a robust numerical solver are crucial for getting accurate solutions.

The applicability of CFD package for determining the flow patterns in a bubble column was tested. The results were compared with the experimental results available in literature and there exists a good agreement between the two.

During the study of flow pattern it was observed that higher gas velocities, higher values of solid loading and lower particle diameter makes the system dynamics faster. The results presented are useful for understanding the dynamics of gas liquid solid flows in bubble column and provide a basis for further development of CFD model for three phase systems

Further, the effect of design variables and process variables on flow pattern in three phase bubble column has been going on. A separate communication will be done on these aspects.

Nomenclature

a – specific gas-liquid interfacial area, $m^2\ m^{-3}$
A – projected area, m^2
A_p – area of a single particle projected in the flow direction, m^2
C_D – Drag coefficient, s^{-1}
d_p – diameter of sinlge particle, m
d_s – sparger diameter, m
D_i – column inner diameter, m
D – Drag force, N
g – gravitational acceleration, $m\ s^{-1}$
H – column height, m
k – turbulence kinetic energy, $m^2\ s^{-2}$
M – momentum exchange term, $kg\ m^{-2}\ s^{-2}$
$n_{P,V}$ – number of particles per unit volume
p – pressure, Pa
R – universal gas constant, $Pa\ m^3\ kg^{-1}\ mol^{-1}\ K^{-1}$
t – time, s
u – superficial fluid phase velocity, $m\ s^{-1}$
$(u_\alpha - u_\beta)$ – relative velocity between two phases, $m\ s^{-1}$
v – velocity, $m\ s^{-1}$
Vp – volume of a single particle

Greek letters

ρ – phase density, $kg\ m^{-3}$
σ – interfacial tension, $N\ m^{-1}$
ν – kinematic viscosity, $m^2\ s^{-1}$
ε – turbulence eddy dissipation, $m^2\ s^{-3}$
ε_α – holdup of phase α
μ – phase viscosity, $kg\ m^{-1}\ s^{-1}$
τ – shear stress, $N\ m^{-2}$
φ – volume fraction, %

Subscripts

α – phase
g – gas phase
l – liquid phase
lam – laminar
s – solid phase
T – transpose
turb – turbulent
1 – gas phase
2 – liquid phase
3 – solid phase

References

1. *Pfleger, D., Gomes, S., Gilbert, N., Wagner, H. G.,* Chem. Eng. Sci. **54** (1999) 5099.
2. *Sokolichin, A., Eigenberger, G.,* Chem. Eng. Sci. **49** (1994) 5735.
3. *Krishna, R., van Baten, J. M., Urseanu, M. I.,* Chem. Eng. Sci. **55** *(*2000) 3275.
4. *Ranade, V. V., Tayalia, Y.,* Chem. Eng. Sci. **56** (2001) 1667.
5. *Mitra-Majumdar, D., Farouk, B., Shah, Y. T.,* Chem. Eng. Sci. **52**(1997) 4485.
6. *Padial, N. T., VanderHeyden, W. B., Rauenzahn, R. M., Yarbro, S. L.,* Chem. Eng. Sci. **55** (2000) 3261
7. *Michele, V., Hempel, D. C.,* Chem. Eng. Sci. **57** (2002) 1899.